Title

Structured Surfaces with Engineered Wettability: Fundamentals, Industrial Applications and Challenges for Commercialization

ISBN

978-3-030-59564-7

Authors

Yang, Woo Seok
Kim, Chang-Jin "CJ"

Publication Date

2021

DOI

10.1007/978-3-030-59565-4_3

Peer reviewed

3. Structured Surfaces with Engineered Wettability: Fundamentals, Industrial Applications and Challenges for Commercialization

Woo Seok Yang[1,2] and Chang-Jin "CJ" Kim[2,3,4]*

[1]Intelligent Sensors Research Section, ICT Creative Research Laboratory, Electronics and Telecommunications Research Institute (ETRI), Daejeon, Republic of Korea

[2]Mechanical and Aerospace Engineering Department, [3]Bioengineering Department, [4]California NanoSystems Institute, University of California, Los Angeles (UCLA), California, USA

* Correspondence: cjkim@ucla.edu, +1-310-825-0267

Abstract

Wettability is a fundamental property used to determine solid-liquid interactions and plays an important role in developing functional materials and devices for many industrial applications. The wettability of a solid surface can be controlled by not only its chemistry but also its roughness. Structured surfaces, such as superhydrophilic, superhydrophobic, and superoleophobic surfaces as well as mixed-zone surfaces, have been explored for self-cleaning, antifouling, anticorrosion, oil-water separation, droplet handling, drug delivery and microfluidics over the past two decades. In this chapter, an overview of recent developments in such wettability-engineered surfaces for industrial applications is provided, focusing on their different strategies or methods and unique competitive advantages. Finally, the main technological challenges for commercialization are discussed.

Keywords: wettability; superhydrophilic; superhydrophobic; application; commercialization

3.1. Introduction

Many industrial applications of conventional and advanced technologies demand materials and devices with certain surface properties to fulfill specific goals. As a fundamental property that describes how a liquid contacts a solid surface, wettability greatly affects the physicochemical interactions between the two. Quantified by the contact angle (CA) of water on them, or water contact angle (WCA), solid materials are hydrophilic or hydrophobic, exhibiting WCA up to 120° [1,2] on their smooth surface. Since wettability is governed by the morphology as well as chemical composition of the surface, the solid surfaces can be roughened to expand their wettability range to superhydrophilic (SHPi) (WCA < 10°) or superhydrophobic (SHPo) (WCA > 150°) regimes [3,4,5]. This approach to extend the water wettability is, in principle, valid for other liquids as well, leading to superoleophobic, superlyophobic, etc. and even superomniphobic. The timely advances in nanotechnology and surface engineering have led to many artificial surfaces with special wettability and provided new functional materials and devices for various industrial sectors.

In this review, first the fundamentals of engineered wettability for its classification, control and fabrication will be summarized. Subsequently, several important surfaces with engineered wettability and their applications along with their current or future markets will be overviewed, focusing on the mainstream examples of technological development and competition. Finally, the main challenges to commercialize the wettability-control technologies will be discussed.

3.2. Fundamentals

3.2.1. Wettability Classification and Terminologies

When a liquid drop is placed on a solid surface in a vapor (or gas), it spreads toward a low energy state of the solid-liquid-vapor system, forming a three-phase contact line. Wettability, i.e., the ability of a liquid to keep contact with a solid surface, is normally quantified by the solid-liquid CA shown in Figure 3.1a. Assuming water for the liquid, a solid surface may be classified as being hydrophilic (CA < 90°) or hydrophobic (CA > 90°) with additional classification of being SHPi (CA < 10°) or SHPo (CA > 150°) to address the unusual wettability of structured surfaces. Incidentally, the definitions of the new terminologies are still evolving, as one can see from the requirement of roll-off (or tilt, sliding) angle or CA hysteresis (CAH) smaller than 5° or 10° being added to the initial requirement of CA > 150° for a surface to be SHPo.

If the liquid is not water, the prefix “hydro-” (meaning water) in the classification terms would change to something else, such as “oleo-” (meaning oil) to say a surface is superoleophobic or super-nonwettable to oil (i.e., with CA > 150°). Because the surface energy of oils (γ = 25-32 mJ/m^2) [6] is much lower than that of water (γ = 73 mJ/m^2), a superoleophobic surface [7] is naturally SHPo as well. An extreme case would be the surfaces that are super-nonwettable to all liquids [8], i.e., superomniphobic ("omni" meaning all) surface, which is naturally superoleophobic and SHPo as well. However, there are exceptional and peculiar wettability properties, such as the surfaces that are superoleophobic and SHPi (i.e., opposite to the natural state of being superoleophilic and SHPo) [9]. Since these newly discovered or designed properties

continue challenging the existing definitions of terminologies to evolve, herein the authors will refrain from delving into the relatively new terminologies.

3.2.2. Rough Surfaces and Moving Liquid

The wetting behavior of a liquid on a smooth surface can be described by Young's equation [10], which balances the interfacial tensions between solid-liquid (γ_{sl}), solid-vapor (γ_{sv}) and liquid-vapor (γ_{lv}) in equilibrium to provide the equilibrium CA (θ_o), as follows:

$$\cos\theta_o = \frac{(\gamma_{sv} - \gamma_{sl})}{\gamma_{lv}} \quad (1)$$

The wetting behavior of a liquid on a rough (e.g., textured) surface can be described similarly by adding the roughness value and depending on whether the liquid fills or sits on the roughness: Wenzel regime [11] and Cassie–Baxter regime [12], respectively (Figure 3.1b). If a droplet is in the Wenzel state, the effective equilibrium CA (θ^*) on rough surface is determined by the roughness factor (r) as well as the equilibrium CA on smooth surface (θ_o), as the following equation [11]:

$$\cos\theta^* = r\cos\theta_o \quad (2)$$

The roughness factor (r) is defined as the ratio of the actual solid surface area to the projected (i.e., looking from top) area. Equation 2 implies the roughness would amplify the inherent wettability; in other words, a wettable surface would become more wettable and a nonwettable surface more nonwettable when roughened. If a droplet is in the Cassie–Baxter state, where the contact surfaces are heterogeneous, i.e., solid-liquid and vapor-liquid, the effective equilibrium CA (θ^*) on rough

surface is determined by the solid fraction (ϕ_{sl}) and the vapor fraction (ϕ_{vl}) as well as the equilibrium CA on smooth surface (θ_o), as the following equation [12]:

$$\cos\theta^* = \phi_{sl}\cos\theta_o - \phi_{vl} \quad (3)$$

where ϕ_{sl} and ϕ_{vl} are the ratios of the solid-liquid and vapor-liquid surface areas to the total surface area, respectively. Equation 3 implies the solid fraction (ϕ_{sl}) would amplify the inherent wettability and the vapor fraction (ϕ_{vl}) would amplify the inherent non-wettability. Note Equation 3 reduces to Equation 2 if $\phi_{vl} = 0$, because it also means $\phi_{sl} = r$. In other words, the Wenzel state is a special condition of the Cassie-Baxter state. If the solid-liquid and vapor-liquid interfaces are both flat as shown in Figure 1(b), the above equation reduces to a more commonly used form, as follows:

$$\cos\theta^* = \phi_{sl}(\cos\theta_o + 1) - 1 \quad (4)$$

Since Cassie-Baxter state is usually metastable and can be transformed into the stable Wenzel state, there is also a transitional state between the two states [13].

As another important parameter to describe the liquid wetting behavior, CAH can be intuitively understood by a droplet resting on a tilted surface [14,15]. Because gravity pulls on the droplet to move it downwards while CAH tries to keep it in place, the droplet deforms to an asymmetric shape with the advancing contact angle (θ_{adv}) at the leading end and the receding contact angle (θ_{rec}) at the following end, as illustrated in Figure 3.1c. The CAH is the difference between them and usually measured by the tilt angle for convenience. The tilt angle, also called sliding angle or roll-off angle, is the angle above which the droplet moves down the inclined

substrate. Note, however, unlike CAH, which is determined solely by the wettability, the tilt angle is not fundamental because it is affected by the volume of the droplet as well.

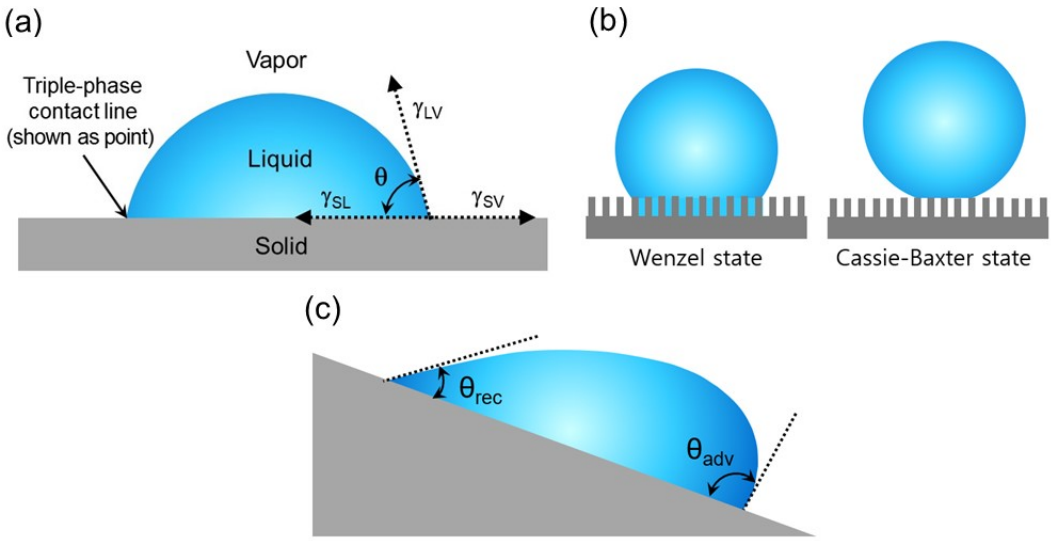

Figure 3.1. Schematics of a liquid droplet showing: (a) contact angle (CA) on a smooth and flat solid surface; (b) two wetting states on a rough solid surface, Wenzel state (left) and Cassie–Baxter state (right); (c) advancing contact angle (θ_{adv}) and receding contact angle (θ_{rec}) on a tilted solid surface.

3.2.3. Wettability Expansion and Control

In general, the wettability of a solid surface can be controlled by the surface chemistry and surface roughness. To obtain a SHPi surface, a high-energy material such as TiO_2 and SiO_2 can simply be roughened [16] because they are intrinsically hydrophilic ($\theta_o < 90°$). To obtain a SHPo surface, usually a material is roughened and coated with a low-energy material, such as fluoropolymer, which is intrinsically hydrophobic ($\theta_o > 90°$). However, it is difficult to obtain a superoleophobic surface because oils would intrinsically wet ($\theta_o < 90$) all materials including

fluoropolymer. Because no known solid surface is intrinsically nonwettable ($\theta_o > 90°$) to the common low-energy liquids (e.g., $\gamma < 30$ mJ/m^2), surface roughness with a reentrant profile (e.g., T-shaped [7], inverse trapezoidal-shaped [17], mushroom-like [8]) have been developed to induce Cassie-Baxter state and an apparent nonwettability. Once induced nonwettable ($\theta^* > 90°$), super-nonwettability ($\theta^* > 150°$) may be obtained by reducing the solid fraction (ϕ_{sl}).

The surface wettability can be dynamically tuned or switched by reversible changes in the surface chemistry and/or the surface morphology in response to corresponding external stimuli, including light, electrical potential, temperature, pH, stress, solvent, and ion [18,19]. The stimuli-responsive surfaces have been developed commonly by using active functional polymers, which can translate a molecular change in charge or dipole or conformation into a change in a macroscopic function such as polarity and roughness [19]. As a special case, a light-responsive surface could be fabricated by using photosensitive materials of oxides (e.g., TiO_2, SnO_2, ZnO, WO_3, V_2O_5 and Ga_2O_3) as well as polymers with photochromic functional groups (e.g., azobenzene, spiropyrane and diarylethene) [18]. The inorganic materials have the advantages of lower toxicity and greater mechanical/chemical/thermal stability but also the drawbacks of slow response and common use of ultraviolet (UV) light irradiation. The organic materials have more advantages with respect to chemical modification and reaction diversity under UV or visible light, in spite of the shortcomings of smaller wettability change and weak mechanical/thermal/radiation stability.

3.2.4. Fabrication Methods for Wettability Engineering

Various fabrication methods have been used to obtain super-wetting and super-nonwetting surfaces. They are, in general, composed of two main procedures – modifying surface chemistry and structuring surface morphology. According to the processing order, they can be classified into three types: pre-roughness post-chemistry, pre-chemistry post-roughness and one-step roughness/chemistry [20]. For example, super-nonwetting surfaces are usually produced as follows. In the first type, substrate surface was etched (with or without lithography) or coated (with particles or fibers) to form rough structures and then chemically modified with silane- or fluorine-containing polymers. In the second type, particles or fibers were first chemically modified and then spray-coated on substrate to generate rough surface. In the third type, chemically modifying layers with rough structures were in-situ synthesized or polymerized onto substrate surface via vapor phase polymerization, electrodeposition, co-condensation, etc.

In terms of how to generate the surface roughness, the fabrication methods can be also categorized into another three types: top-down, bottom-up and combination approaches [21]. For top-down approach, rough surface structures were produced by etching (with or without lithography) or templating. For bottom-up , coating or self-assembly was commonly used. For the combination, surfaces with hierarchical roughness were obtained in two steps of top-down fabrication for microstructures and bottom-up fabrication for nanostructures.

3.3. Applications

3.3.1. Self-cleaning

Self-cleaning surfaces and coatings are used mainly for glasses in building, cars and solar panels, but also for paints and textiles. The self-cleaning coatings have been developed through two categories of SHPo and SHPi films [22]. A self-cleaning SHPo surface cleans itself by letting a water droplet roll over the rough surface in Cassie-Baxter state. Since most particles (dirt) are hydrophilic, the rolling water droplet picks up and carries the particles with it, as illustrated in Figure 3.2a. In comparison, a self-cleaning SHPi surface can also clean itself by letting water sheet over the rough surface in Wenzel state. If the roughness scale is smaller than the particle scale, the adhesion between the particles and solid surface is relatively small so that the sheeting water picks up and carries the particles with it, as illustrated in Figure 3.2b.

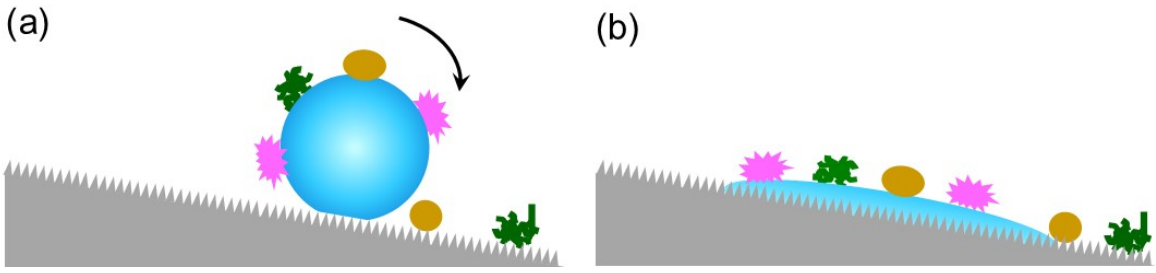

Figure 3.2. Schematic illustration of self-cleaning processes on: (a) SHPo and (b) SHPi surfaces.

The most common type of SHPo coating is created by using hydrophobic fumed silica (SiO_2) particles, whose surface has been modification with silicone oil or functional silanes such as dichlorodimethyl silane (DDS), hexamethyldisilazane (HMDS), polydimethylsiloxane (PDMS) or octametylcyclotetrasiloxane (D4) [23]. By a facile technique of dip or spray coating, it was

easily coated as a SHPo film with rough porous surface originated from the aggregated nanoparticles (NPs). Self-cleaning of this type of SHPo surfaces was demonstrated on various practical substrates, such as window glass, building wall, solar cell panel, motorcycle body, clothing fabrics, cotton shoes, wood, marble, etc. [24]. The sprayable SHPo coatings based on the hydrophobic fumed silica have been commercialized as multiple products (e.g., AEROSIL®, CAB-O-SIL®, HDK®, NeverWet®, Ultra-Ever Dry®) due to cost-effective production capability as well as the additional performance benefits such as optical transparency, scratch/abrasion resistance, corrosion resistance and reduced moisture adsorption.

Self-cleaning SHPi coatings are mostly based on titania (TiO_2) with both photoinduced hydrophilic conversion and photocatalytic properties [16,22]. Rough titania surfaces can turn from hydrophilic to SHPi under UV radiation, which changes the valence of Ti^{4+} to Ti^{3+} with the release of O_2, followed by water occupation of the oxygen vacancies [25]. The UV radiation also generates electron-hole pairs on the TiO_2 surface to react with water and oxygen into reactive oxygen species (such as $\cdot OH$ and $O_2^{\cdot -}$), which can decompose organic pollutants into harmless CO_2 and H_2O [26,27]. Stronger photocatalytic and SHPi properties can be obtained by using anatase with an open crystal structure (vs. densely packed rutile phase) and increasing NP concentration due to the larger specific surface area [16,22]. Although ZnO and SnO_2 also have both photoinduced hydrophilicity and photocatalysis [26], TiO_2 is much more preferred for commercial products (e.g., Pilkington Activ™, Sun Clean Glass®, NEAT®, HYDROTECT®, Bios Self-Cleaning®, SGG BIOCLEAN®) because of non-toxicity, high chemical/thermal stability and low cost.

For self-cleaning applications, TiO_2-based SHPi coatings are more extensively utilized than SiO_2-based SHPo ones because the former can also have antifogging, antireflective, deodorizing and antibacterial properties [16,26]. Furthermore, their self-cleaning activity can be further improved through chemical modifications. TiO_2-coated surfaces typically lose the SHPi property within minutes to hours in dark without UV radiation (only 3–5 % of sunlight) [16], limiting their practical applications. This critical drawback could be overcome by metal ion doping (Cu, Fe, Co, Sn or V), noble metal loading (Ag, Au or Pt), non-metal doping (N, S or C) or hybrid nanocomposite (apatite/TiO_2, Fe_3O_4/TiO_2, carbon nanotube (CNT)/TiO_2 or Cu/TiO_2/C.) [27]. The high bandgap of TiO_2 (~3.2 eV) can be narrowed to absorb visible light by introducing additional energy levels within the band gap and heterojunction coupling. The modified TiO_2 NPs showed photocatalytic antibacterial activity in response to visible light illumination.

3.3.2. Antifouling

Fouling is the accumulation of undesirable materials on a solid surface, causing functional degradation by physical and/or chemical interactions between them. In a marine environment, foulants are micro-organisms (bacteria, diatoms, etc.) and macro-organisms (macroalgae, mussels, barnacles, etc.) [28]. The biofouling roughens the surface and increase the drag of a ship moving through water, consequently raising fuel consumption and greenhouse gas emission. Antifouling coatings are estimated to save the shipping industry $60 billion in fuel consumption and reduce 384 and 3.6 million tonnes in CO_2 and SO_x emissions, respectively [29]. For marine application

with the biggest portion of antifouling coating market, the most well-known is the self-polishing copolymer (SPC) containing dicopper oxide (Cu_2O) as the main biocide along with booster biocides [28]. As the international regulations on marine environment are tightened, fouling release coating (FRC) has been focused on as a new eco-friendly technology that is copper-free, biocide-free and metal-free. Two main approaches of FRC are the detachment of settled biofoulants on hydrophobic surface by hydrodynamic stress during ship navigation (Figure 3.3a) and the prevention of biofouling attachment on hydrophilic surface by keeping it hydrated (Figure 3.3b) [30]. The first approach uses polymer materials with low surface energy and low elastic modulus such as polysiloxanes and fluoropolymer. With ~23 mJ/m^2 of surface energy and 2 MPa of elastic modules [31], PDMS is most widely used for commercial products including Hempasil® 77500, Intersleek® 700, SigmaGlide® 990 and Surface Coat (Duplex Fouling Release System) [28]. The second approach uses polymers with much higher surface energy to retain a permanent hydration layer which prevents the adhesion of proteins, the triggering process of biofouling attachment, by providing very low interfacial energy between water and a surface. The most commonly used is poly(ethylene glycol) (PEG), which has a high surface energy (> 43 mJ/m^2) and low water interfacial energy (< 5 mJ/m^2) [30]. The first approach (i.e., hydrophobic FRC) is commercially more successful than the second approach (i.e., hydrophilic non-stick FRC) because of the higher performance proven except under no or slow water flow. The drawbacks of PDMS, i.e., poor adhesion and mechanical durability, could be improved by incorporating inorganic filler

(SiO_2, $CaCO_3$, TiO_2, Fe_2O_3 or carbon black) and polymer segments (epoxy or polyurethane (PU)) [30,32].

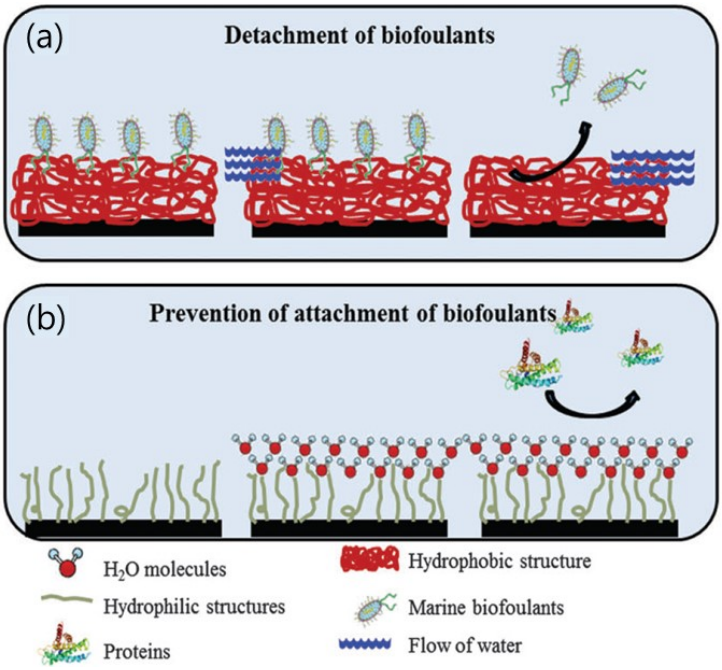

Figure 3.3. Schematic illustration of fouling release coating approaches for marine application: (a) hydrophobic coating to detach settled biofoulants by hydrodynamical stress during ship navigation; (b) hydrophilic hydrating coating to prevent attachment of biofoulants. Reproduced from reference [30].

Biomedical application is an emerging area of antifouling coatings for future markets. The surface fouling of biomedical devices by protein and microbial attachment is responsible for a significant portion of healthcare-acquired infections (HAIs) [33], which result in 1.7 million infections and 99,000 associated deaths each year [34]. Two strategies are used to prevent the device-associated HAIs: one is an antimicrobial material to kill microorganisms or inhibit their

growth through biocide release or contact kill, and the other is an antifouling coating to prevent protein and bacterial adhesion [33]. For the biomedical antifouling, hydrophilic PEG-based coatings have been more widely investigated than SHPo coatings, which easily become SHPi under usage in practice.

Like biomedical applications, consumer electronics including displays and touch panels is a niche market for antifouling coatings. High anti-fingerprint (AF) performance has been demonstrated by various oleophobic surfaces with hierarchical or reentrant structures, but the complex surface structures are inconvenient for low-cost manufacturing in industrial scale [35]. AF coating can be more efficiently accomplished by a facile method using transparent polymers with low surface energy and strong mechanical durability on glass such as perfluoropolyether (PFPE) [36].

3.3.3. Anticorrosion

Corrosion is a natural slow process that destructs materials (usually metals) by converting them into a more chemically stable form (such as oxide, hydroxide or sulfide) through a chemical and/or electrochemical reaction with their environment, resulting in functional damage on bridges, cars, water heaters and countless other products. The global cost of corrosion was estimated to reach 2.5 trillion USD, which was equivalent to 3.4 % of the global gross domestic product (GDP) in 2013, and 25–30 % of the cost could be saved by employing optimum corrosion management practices [37]. Metal corrosion proceeds via two different processes, the movement of metal ions

into solution on active areas (anodes) and passage of electrons from a metal to an acceptor (such as oxygen, hydrogen ions or another oxidizing agent) on less active areas (cathodes) [38].

In accordance with the protective mechanism, anticorrosion coatings are generally classified into three types: sacrificial, barrier and inhibitive coatings [39]. Sacrificial coatings use an electrochemically more active metal pigment (most commonly 92–95 wt% zinc), which corrodes preferentially to protect the surface from corroding by cathodic protection (or galvanic effect). Barrier coatings consist of polymer binder (e.g., epoxy, urethane, acrylic, alkyd) and inert inorganic pigment (e.g., TiO_2, micaceous iron oxide of Fe_2O_3, glass flakes) at a lower volume concentration, resulting in dense and cohesive coatings that impede the transfer of aggressive species (liquids, gases and ions) into the coating-substrate interface. When inhibitive coatings are permeated by moisture, the inhibitive pigments of slightly water-soluble inorganic salts (e.g., phosphates, chromates, molybdates, silicates) are partly dissolved and carried into the coating-substrate interface, forming a passivation layer by the reaction of dissolved ions with substrate. Barrier coatings are most widely used because they can be used for immersed environments (underwater or buried in soil) as well as for marine and industrial atmospheres. Furthermore, they can be applied for primer, intermediate coat and topcoat of multilayered systems, while the others can be only for the primer on substrate. With increasing environmental regulations against volatile organic compounds (VOCs) emissions [40], waterborne acrylic and inorganic powder coatings are currently focused on as eco-friendly anticorrosion technologies. Inorganic powder coating is more beneficial due to superior durability, scratch resistance, gloss retention and resistance to chalking.

Superhydrophobic coatings have been developed for a new high-performance anticorrosion technology, because the air trapped in the surface roughness under water can effectively isolate the substrate from aqueous corrosive media (Figure 3.4a) and the water forms droplets (rather than an electrolyte film) in humid air, suppressing the electrochemical reaction (Figure 3.4b) [41]. Inorganic NP-based coatings are especially promising for an environmentally-friendly and mechanically-durable anticorrosion. Common examples are silane-modified oxide NPs and polymer/inorganic NP composites. The former imparted superhydrophobicity on metal surfaces by combining low surface energy of silane or fluorosilane with surface roughness of oxide NPs such as silica (SiO_2) [42] and zeolite (SiO_2/Al_2O_3) [43]. The latter was composed of polymer bases and embedded inorganic NPs such as polytetrafluoroethylene (PTFE)/SiO_2 [44], PU/Al_2O_3 [45] and epoxy/graphene [46]. The latter is more advantageous for high mechanical durability because the polymer base can improve the cross-liking of NPs and the adhesion with substrate.

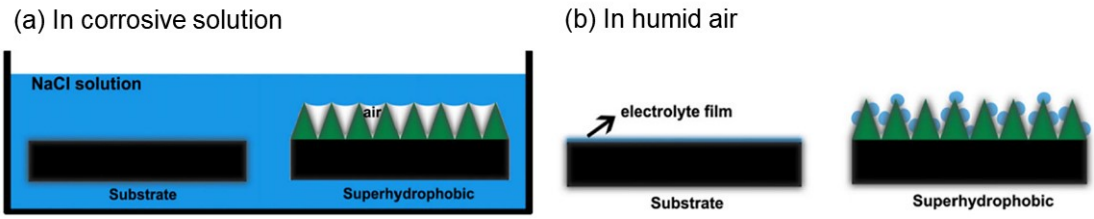

Figure 3.4. Schematic models to explain corrosion resistance on SHPo surfaces in: (a) corrosive solution and (b) humid air. Reproduced from reference [41] with permission from Elsevier.

To compete with the conventional anticorrosion coatings, SHPo coating should have high mechanical durability for long-lasting performance as well as high corrosion resistance. Some

methods have been researched to improve the durability of SHPo coating such as self-healing ability after mechanical damage, mechanically robust surface with hierarchical structures and multiple hybrid coatings consisted of inhibitor-doped primer and SHPo topcoat [47]. Meanwhile, conventional barrier coatings have been modified with siloxane having strong Si-O bonds or polyaniline (PANI) as a conductive filler, resulting in increased resistance against mechanical wear, weathering or delamination [48]. It is still unclear whether SHPo anticorrosion coatings can have a better mechanical durability than conventional anticorrosion coatings. The authors are not aware of any published research work on this issue to date. Moreover, it is not clear if the SHPo property can be maintained under service because SHPo surfaces easily become SHPi in practice.

3.3.4. Oil-Water Separation

Many industries (mining, petrochemical, metal/steel, textile, food, etc.) produce massive amount of oily wastewater every day, and frequent oil spill accidents cause serious environmental pollution. To address these issues, a variety of oil-water separation methods have been used, such as gravity or centrifugal settling, bioremediation, electrochemical, coagulation and air floatation [49]. A simple and cost-effective method is filtration and absorption technology using meshes/membranes and 3D porous materials (sponges, foams, textiles or aerogels) [50]. Meshes or membranes are used to separate immiscible or emulsified oil-water mixtures, while 3D porous materials are used to quickly absorb oil in lakes, rivers or oceans without any specialized equipment for emergency response of oil spillage. Special wetting materials have been researched

to develop advanced filters and absorbents with high separation efficiency and high flux rate or absorption capacity.

Two types of meshes/membranes with specific wettability are applied for filtration: one that blocks water and passes oil through because it is both SHPo and superoleophilic (Figure 3.5a) and another that passes water through and blocks oil because it is both SHPi and superoleophobic (Figure 3.5b) [51]. The first type is not suited for gravity-driven separation of light oils from immiscible mixtures of oil and water because water will sink below the light oil to form a thick underlayer preventing the oil from continuing to pass through the mesh [52]. Moreover, the viscous oils easily adhere to the mesh and impedes its flow, significantly decreasing the flux rate of oils. The second type can overcome this deficiency and provide advantages for some applications such as fuel purification, oil fence for an oil spill accident and separation of high viscosity oils [49]. Hydrophilic materials with micro/nano-hierarchical surface structures can show superhydrophilicity and underwater superoleophobicity in oil-water mixtures because water molecules are trapped in the rough surface structures to repel oil droplets from adhering onto the water-solid composite surface. Typical water-passing meshes have been fabricated by coating metal meshes with nanostructured materials such as hydrophilic oxides ($Cu(OH)_2$, CuO, TiO_2, SiO_2/Al_2O_3 or graphene oxide) [50], hydrophilic hydrogel (polyacrylamide (PAM) [53] or poly(3,4-ethylenedioxythiophene):poly(styrenesulfonate) (PEDOT:PSS) [54]) and hydrophilic-oleophobic synthetic or blended polymers (poly(diallyldimethylammonium chloride)-

pefluorooctanoate (PDDA-PFO) [55] or fluorodecyl polyhedral oligomeric silsesquioxane (F-POSS)/cross-linked poly(ethylene glycol) diacrylate (x-PEGDA) [49]).

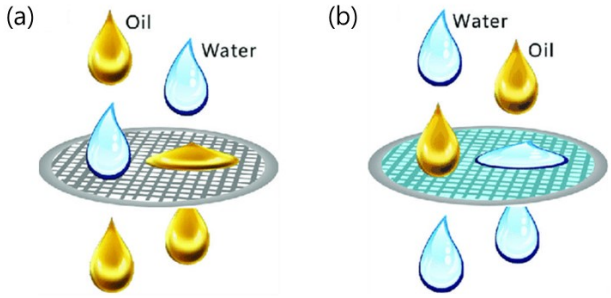

Figure 3.5. Schematic illustration of oil-water filtration mesh: (a) oil-pass type mesh that is both SHPo and superoleophilic and (b) water-pass type mesh that is both SHPi and superoleophobic. Reproduced from reference [51] with permission from PCCP Owner Societies.

Membranes with small pores (< ~1 μm) are more suitable than meshes to separate oil-water emulsions (e.g., 1 wt% oil-in-water or 1 wt% water-in-oil) [50], where oil or water droplets are much smaller than those in immiscible oil-water mixtures. Polymer membranes are much more widely used than ceramic ones due to low cost, superior chemical/mechanical stability and highly integrated operation [56]. An oil-passing poly(vinylidene fluoride) (PVDF) membrane that is both SHPo and superoleophilic could separate both nano-sized surfactant-free and surfactant-stabilized water-in-oil emulsions with high separation efficiency (> 99.95 wt%) and flux rate (several times higher than those of commercial filtration membranes) [57]. In comparison, water-passing membranes that are both SHPi and underwater superoleophobic can have much better antifouling property and resulting recyclability due to the ultralow oil adhesion. Water-passing PVDF

membranes have been fabricated by surface grafting with a zwitterionic polyelectrolyte brush (poly(3-(N-2-methacryloxyethyl-N,N-dimethyl) ammonatopropanesultone (PMAPS) [58] and PEGDA [59].

The conventional absorbents are commonly used to remove oil spill from water, including inorganic minerals (zeolite, silica aerogel, expanded vermiculite, clay, activated carbon), synthetic porous polymers (nonwoven polypropylene (PP), melamine (MA), PU foam) and natural fibers (cotton, wool, milkweed, etc.) [49]. Their separation efficiency and oil absorption capacity could be improved by hydrophobic surface modifications, as in the examples of fluoro- or alkyl-modified silica aerogel [49], CNT/nanofiber coated vermiculite [49], organically modified clays (with inorganic cations replaced with organic cations) [49], dodecanoic acid–copper particle coated PU foam [60] and polymerized octadecylsiloxane (PODS) coated MA sponge [61]. As another approach to obtain advanced absorbents, novel synthetic porous materials have been developed, including inorganics (CNT sponge [62], twisted carbon fiber aerogel [63], graphene–CNT aerogel [64], silicon sponge [65]), organics (nanoporous poly(divinylbenzene) (PDVB) [66], methyltriethoxysilane (MTES)-dimethyldiethoxysilane (DMDES) aerogel [67], supermacroporous polystyrene (PS) monolith [68]) and organic-inorganic hybrid or composite (fluorinated metal–organic framework (MOF) [69], PVDF/camphor soot NP composite [70]).

In addition to good performance, environmental friendliness is another important factor in developing advanced materials for oil-water separation, especially in the case of absorbents with a shorter service life than filters. Nanocellulose (NC)-based oil absorbents have been fabricated,

such as TiO_2-coated NC aerogels [71] and octyltrichlorosilane (OTCS)-modified NC aerogels [72], because NC is a low-cost, renewable and biodegradable material [49]. Reusable oil absorbents have also been fabricated with magnetic-controllable special wetting materials, which consist of magnetic materials (Fe, Fe_2O_3, Fe_3O_4) and hydrophobic/oleophilic materials (carbon materials, organoclays, polymers) [49,50]. These particles could float on contaminated water to absorb spilled oil and could be collected after oil absorption by applying an external magnetic field. The absorbed oil could be readily removed from the particle surfaces by a simple ultrasonic treatment and the particles still retained their highly hydrophobic/oleophilic characteristics.

3.3.5. Droplet Handling for Biomedical Analyses

Molecular diagnostics is one of the most important tools to analyze pathogen biomarkers due to its high sensitivity and specificity. Biological fluids (blood, serum, plasma) are the main sources of biomarkers but contain an extremely small number of biomarkers in the early stage of many diseases. For successful diagnosis of a small volume biofluid (10^1-10^3 nl), a novel handling technique without a sample holder has the advantages of eliminating the wall adsorption and avoiding the contamination induced by the sample-wall interaction [73]. Ultrasonic levitation is currently used for contactless analyses of liquid droplets [74,75] but has the limitations of complex experimental setup, bulky transducer and high cost. Superhydrophobic surfaces have emerged as a simple low-cost method of contactless liquid handling due to their ability to minimize the liquid-surface contact area and resultant sample contamination [73].

Liquid holders with SHPo (i.e., nearly contactless) surface were fabricated with an array of micro/nano-sized Si pillars, whose top surfaces were modified by silanization to impart superhydrophobicity [76] or by Ag nanoparticle incorporation and subsequent hydrophobic polymer coating to attain surface enhanced Raman scattering (SERS) effects as well as hydrophobicity [77]. Liquid sample droplets on the surfaces exhibited the Cassie-Baxter state, greatly reducing the effective contact area and contamination. Furthermore, the droplet could be effectively evaporated to reduce its volume while maintaining the quasi-spherical shape, concentrating the biomarker by 10^2-10^3 [73]. The droplet position could be controlled by introducing a hydrophilic region within the SHPo surface to improve the sample stability during experimental setup such as x-ray beam alignment (Figure 3.6a) [76]. These contactless droplet handling techniques have been applied to many diagnostic tools such as SERS, Fourier transform infrared spectroscopy (FTIR), X-ray diffraction (XRD), X-ray fluorescence (XRF) and X-ray phase contrast imaging (XPCI).

High-throughput screening (HTS) is a primary experimentation method used in biomedical research, especially for drug discovery. A microplate with an array of wells is still commonly used as liquid sample carrier for automated HTS systems in industries despite its drawbacks of high consumption of valuable samples or expensive reagents. Droplet microarray on patterned SHPi/SHPo surfaces can be a new miniaturized platform for HTS of biomedical samples such as blood, cell, protein and biomaterial [73,78]. Grid-like arrays of SHPi spots confined by thin SHPo barriers have been produced on different substrates by a variety of fabrication methods. For an

example, a SHPi, biocompatible and transparent nanoporous film of poly(2-hydroxyethyl methacrylate-co-ethylene dimethacrylate) (HEMA-EDMA) was coated on a glass plate and a SHPo barrier pattern was formed by photografting of 2,2,3,3,3-pentafluoropropyl methacrylate (PFPMA) brushes (Figure 3.6b) [79]. Another example is when a smooth surface of PS substrate was roughened by phase separation methodology to make it SHPo, and SHPi areas were patterned by exposing UV/ozone irradiation [80]. Dense arrays of micro/nanoliter droplets [80,81] have demonstrated appropriate performances for diverse biomedical screening systems of biomaterial-body fluid interaction and cell-cell/cell-protein/cell-biomaterial interactions [78]. Bioactivity of different inorganic NPs could be reliably tested under exactly same conditions by dispensing and drying NP suspensions onto SHPi regions and then immersing the entire chip in simulated body fluid [82]. Multiplexing test of protein-cell interaction could be performed for various independent combinations with different compositions and total concentrations of a binary protein system by sequential processes of first dispensing protein solution, allowing reaction for protein adsorption and washing chip and then dispensing culture medium, reaction for protein-cell interaction and washing chip [80].

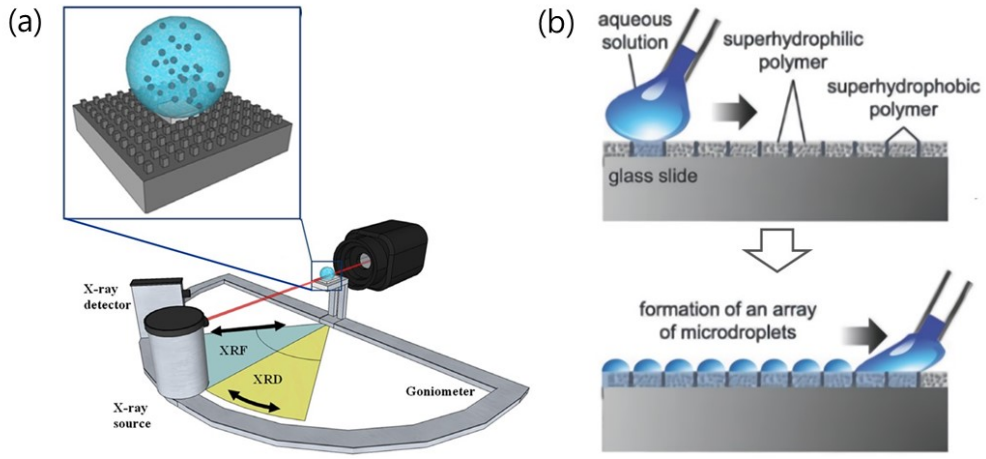

Figure 3.6. Schematics of patterned (super)hydrophilic/SHPo surfaces used for: (a) combined measurements of X-ray fluorescence (XRF), phase contrast imaging (XPCI) and diffraction (XRD). Reproduced from reference [76] with permission from Elsevier. (b) single-step spontaneous formation of a high-density array of completely separated microdroplets. Reproduced from reference [79] with permission from The Royal Society of Chemistry.

3.3.6. Drug Delivery System

A drug delivery system (DDS) is a formulation or a device that transports therapeutic substances into the body, and conventional DDSs have evolved into smart DDSs to enhance the therapeutic efficiency of drugs. Smart DDSs should release drug at specific target site in a controlled manner for a necessary period to reduce drug concentration fluctuation, dosage frequency, drug toxicities and side effects [83]. One of key elements for smart DDSs is controlled-release technology by which drug can be released at a constant rate for a prolonged time. In many cases, the release of therapeutic agent relies on interfacial properties between the DDS and the

biological environment through which the mass transport occurs. Thus, wetting properties of DDS surfaces have a great influence on drug releasing behavior.

Three-dimensional (3D) SHPo mesh can be used as a novel matrix of prolonged and local DDS for long-term treatment of pain and chronic diseases [84]. Biocompatible poly(ε-caprolactone) (PCL) microfibers were electrospun to form a porous bulk mesh, whose hydrophobicity was increased by doping of poly(glycerol monostearate-co-ε-caprolactone) (PGC-C18). When the 3D SHPo mesh was exposed to the aqueous release medium, water penetrated into it in a timely manner to displace its entrapped air (Figure 3.7). The air acted as a removable barrier component within the 3D SHPo mesh, effectively slowing drug release that can occur only at the mesh-water interfaces. The releasing rate could be tuned by the design parameters (mesh thickness, fiber size, hydrophobic doping amount) for structural geometry and surface roughness of the mesh [83,84]. Electrospun polymer fibers were very suitable to fabricate 3D SHPo mesh-based DDSs due to their high drug loading (up to 60%), high encapsulation efficiency (up to 100%), polymer diversity to physico-chemically distinct agents, process simplicity and cost-effectiveness [85].

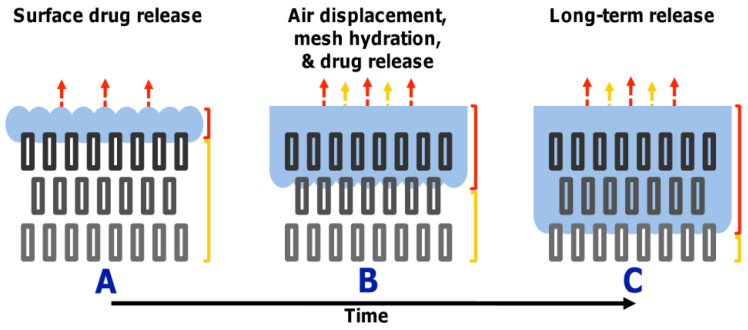

Figure 3.7. Schematic explaining the time-controlled drug release of 3D superhydrophobic mesh. Reproduced from reference [84] with permission from the American Chemical Society.

Stimuli-responsive release has been widely used to achieve controlled-release, and a DDS surface could be switched from SHPo to SHPi [86]. A light-triggered DDS was fabricated with mesoporous silica nanoparticles (MSNs), whose surface was made SHPo with single molecule layer of octadecyltrichlorosilane (OTS) and switched to be SHPi by decomposing the OTS with UV irradiation [87]. The change of MSNs surface from SHPo (closed) to SHPi (open) state was followed by drug release from MSNs' pores. An ultrasonic-controlled DDS was developed with a dense vertical array of titanium oxide nanotubes (TNTs), whose surface was converted to be SHPo by a fluorination with 1H,1H,2H,2H-perfluorooctyltriethoxysilane (POTS) [88]. Ultrasonication could remove the air layer trapped on the surface of SHPo TNTs array, leading to the release of loaded drug. Ultrasound may be a better trigger than light due to the ability to focus precisely into the target region deep under the skin.

Superhydrophobic surfaces can be applied to a fabrication tool for DDSs as well as to DDSs themselves. They were used as an innovative platform for more efficient and cost-effective processes to produce various particles of spherical shape, which is the most commonly employed geometry for particle-based DDSs [78]. Aqueous solutions containing polymeric precursor and bioactive agent were dispensed onto SHPo surfaces by a micropipette, and the liquid droplets were hardened to form spherical particles through chemical cross-linking or solvent evaporation. High encapsulation efficiency (up to 100%) could be accomplished due to the negligibly small droplet-

surface contact area and the absence of a surrounding liquid medium, to which the encapsulated molecules may be easily diffused and lost.

3.3.7. Microfluidics

Microfluidics is a core building block for many biochemical applications, especially for point-of-care testing (POCT). Microfluidic devices generally consist of structural components for the manipulation (e.g., moving, stopping, mixing, separating, filtering) of liquid sample and/or reagents in microchannel networks. They are divided into many different types according to liquid form, liquid driving force and fabrication materials/methods, but regardless of the type, control of surface wettability can play an important role in enhancing their functional performances.

A microchannel with SHPo walls can reduce pressure drop of the liquid flowing in it, resulting in smaller pump, less power consumption and low cost. The air trapped inside the structures on a submerged SHPo surface allows liquid flow with an effective slip, whose amount is generally determined by the surface structures, resulting in a reduction of drag. The drag reduction effect becomes larger as the channel becomes smaller, favoring microchannels over regular-size channels. However, since SHPo surfaces capable of inducing a larger slip are in general more vulnerable to losing its trapped gas [89], the SHPo walls of microchannel should be designed accordingly, considering the tradeoff between drag reduction and robustness in a wide range of flow rate [1]. Capillary-induced microfluidic devices have the advantages of low resource settings, no power consumption and low cost, compared with active types of pressure-driven,

electrokinetic and centrifugal devices. Hydrophilic microchannels are used for capillary pumping (i.e., wicking), and (super)hydrophobic patches incorporated in the hydrophilic microchannel act as a passive valve [1]. Performance (i.e., opening pressure) of the hydrophobic valve was mainly determined by geometric design (height, width) and fine-tuned by the surface nanostructures (spacing, height) [90]. Open microfluidic devices have been explored for low-cost POCT devices by using cheap substrate materials (polymer, paper, textile) due to their advantages of simple and low-cost fabrication as well as easy introduction of liquid sample and reagent. The wettability contrast of (super)hydrophilic/SHPo patterned surface could induce a surface tension-driven force controlling the liquid flows in open microfluidics [91]. The SHPi paths of liquid flow could be patterned on SHPo substrates as the following examples. Superhydrophobic surface was formed on PS substrate by phase separation technique, and then SHPi paths were created by a UV/ozone or plasma exposure through a photomask [92]. Superhydrophobic paper was obtained by surface precipitation of polyhydroxybutyrate (PHB) and hydrophilic channels were patterned by argon plasma treatment [93].

Unlike continuous flow microfluidics, digital microfluidics is based on the manipulation of individual droplets on a surface for the advantages of less reagent consumption, fast response rate and parallel processing capability. Only by using gravity force, basic manipulations of droplets (e.g., moving, stopping, mixing) could be accomplished on SHPo anodized aluminum oxide (AAO) surface with hydrophilic polydopamine micropatterns (channels, patch) [94]. For accurate and complex manipulations, droplets have been actuated by different methods of electrical field,

optical force, surface acoustic wave (SAW), thermocapillary and magnetic field [95]. The most well-known actuation technique is electrowetting-on-dielectric (EWOD), where a droplet is placed on a hydrophobic dielectric surface between two imbedded electrodes and actuated by the voltage applied between them [96], as drawn in Figure 3.8. Efforts have been made to operate EWOD on SHPo surfaces, anticipating such combination would enhance the EWOD effect and expand microfluidic functionalities [97].

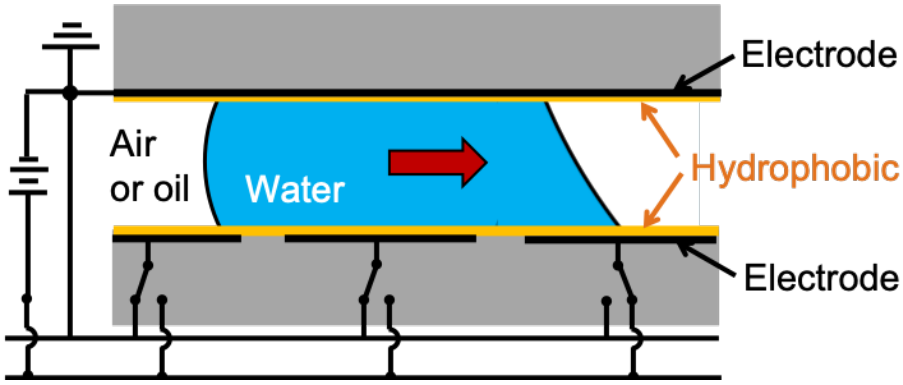

Figure 3.8. Droplet actuation by electrowetting-on-dielectric (EWOD), illustrated with the common device configuration of two parallel plates.

3.4. Challenges

3.4.1. Mechanical Durability

Mechanical durability is one of the critical challenges for many practical applications (self-cleaning, anti-fouling, anticorrosion, oil-water separation, etc.) of most structured surfaces. More vulnerable are SHPo surfaces because they usually employ a soft polymer material and protruding

(i.e. pillar-like) structures, compared with SHPi ones which usually employ a hard material and depressed (i.e., hole-like) structures. The primary durability performance of SHPo coating is in general determined by adherence to substrate, resistance to abrasive force and dynamic impact and stability in dynamic liquid bath condition [98]. Some strategies have been developed to improve the mechanical stability of SHPo surface for a long life time [99,100].

A simple and straightforward method is to directly generate surface topography from hydrophobic bulk material with mechanical durability. But it is very difficult to find non-polymer hydrophobic material because most ceramics and metals are hydrophilic. An alternative approach is to use organic-inorganic composite materials composed of hydrophobic polymers and mechanically durable ceramics or metals. A SHPo composite film was fabricated by blending fluoro-methacrylic latex with montmorillonite clay NPs, whose surface was modified by anaerobic acrylic adhesive, and demonstrated to remain SHPo after dynamic impacts [101]. A crosslinked PDMS matrix containing hydrophobic silica NPs, whose surface was modified by fluorinated alkyl silane (FAS), showed remarkable mechanical durability against repeated machine washes, severe abrasions and boiling water as well as excellent corrosion resistance to strong acid or base [102].

Dual scale surface roughness is a common method to preserve the Cassie-Baxter state even after some surface features are mechanically worn out [99]. The hierarchical-structured surfaces with dual scale roughness consisted of microscale topography for mechanical robustness and superimposed nanoscale roughness for SHPo property. A hierarchical SHPo Si surface was produced by two-step etching processes to form micro-sized pyramids and nanostructures on their

surfaces, followed by perfluorooctyl trichlorosilane (PFOS) treatment for surface fluorination [103]. Compared with Si surface with only the nanostructures, it exhibited less degradation of CA and CAH properties after abrasion test. Interestingly, while poly(ethylene terephthalate) (PET) fabric coated with polymethylsilsesquioxane (PMSQ) nanofilaments retained a low water sliding angle after abrasion test, a glass slide coated with the same PMSQ lost its SHPo property [104].

Self-healing material is an emerging strategy to attain mechanical durability by making an autonomously repairable SHPo surface [99]. A layered porous flexible polymer film containing a large amount of absorbed FAS hydrophobic surfactant could restore superhydrophobicity after mechanical or chemical damage, such as a surface scratch or decomposition of fluoroalkyl chains [105]. The self-healing mechanism was explained by the migration of absorbed healing agent onto the surface in the presence of humidity to minimize its surface energy. An anticorrosion coating based on both a benzotriazole (BTA) corrosion inhibitor and an epoxy-based shape memory polymer (SMP) could rapidly heal the damage of surface morphology (crushed areas or scratches) through a mild heat treatment at 60 °C for 20 minutes or in sunlight for 1 hour [106].

The combination of the individual methods described above is another strategy to develop a mechanically durable SHPo surface. An epoxy/CNT composite hierarchical structure was produced by spray coating of epoxy/CNT/acetone mixture on a micropatterned epoxy surface and by thermal annealing for strong bonding between CNT and substrate [107]. It showed no significant deterioration in CA and CAH properties after long-term exposure to water or exposure to high water pressure, but the similar hierarchical structures using lotus wax instead of CNT lost

superhydrophobicity. A self-healing hierarchical-structured composite was fabricated by sequential spray coatings of epoxy resin base, PS/SiO_2 core/shell NPs and PDMS hydrophobic interconnection as shown in Figure 3.9 [108]. It could maintain SHPo properties (CA > 150 ° and CAH < 10 °) after several sand impacts and automatically restored the SHPo properties after air plasma damage by releasing hydrophobic PS through thermal curing at room temperature for 12 hours or at 150 °C for 1 hours.

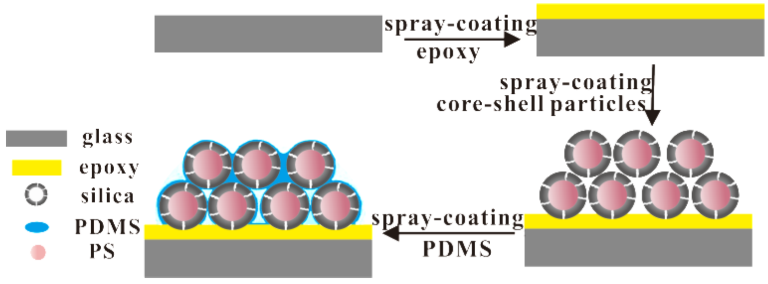

Figure 3.9. Schematic explanation of how a SHPo surface with self-healing hierarchical-structured composite is fabricated. Reproduced from reference [108] with permission the Royal Society of Chemistry.

3.4.2. Scalable Manufacturing

Although various methods have been successfully demonstrated to fabricate structured surfaces in small quantities for characterization and evaluation purposes, scalable manufacturing is still a key barrier for commercialization of the R&D results. It requires the fabrication at industrially relevant scale and low cost, with sufficient production yield and reproducibility while also within environmental, health and safety guidelines [109]. For low-cost large-area processing, solution-based coating (sol-gel, electrospinning, electrochemical deposition, etc.) is more

preferable than vapor deposition, and nanoimprint or self-assembly lithography is better than conventional photo or electron-beam lithography. For scalable industrial production, it is suitable to employ processes such as continuous roll-to-roll (R2R), self-assembly and one-step spray coating. Based on R2R nanoimprinting, a large-area SHPo antibacterial film could be continuously manufactured by using a hierarchical-structured mold of poly(2-hydroxyethyl methacrylate) (PHEMA) and a flexible PET substrate coated with UV-curable photoresist containing ultralow surface energy monomer of 1H,1H,2H,2H-perfluorodecyl acrylate (PFDA), as shown in Figure 3.10a [110]. Without any patterned mold, a double-roll based process could coat SHPo film with shark-skin-like roughness on the roll at the lower rotating speed (#1 Roll at V_1) by using a high viscosity paste comprised of multiwalled CNTs dispersed in PDMS matrix, as shown in Figure 3.10b [111].

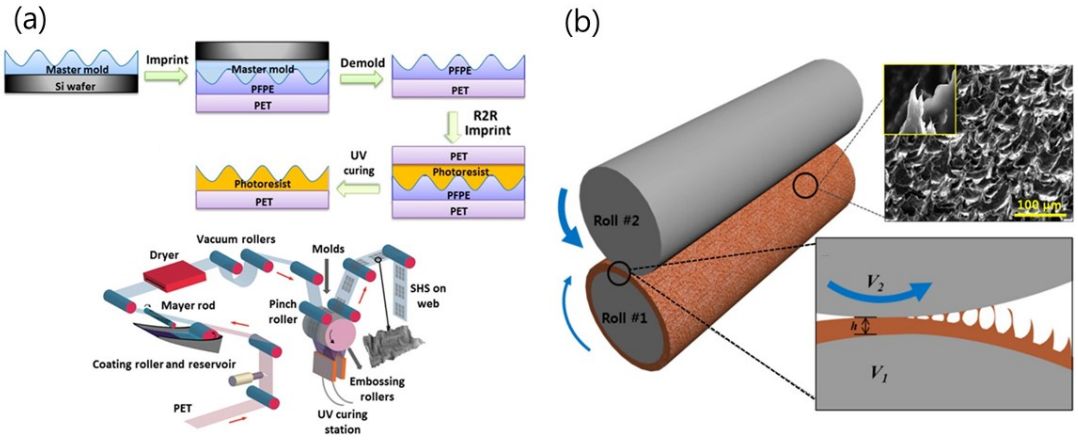

Figure 3.10. (a) Schematics of R2R nanoimprinting processes to fabricate a large-area SHPo antibacterial film. Reproduced from reference [110] with permission from the American Chemical

Society. (b) A double-roll based coating process to fabricate a shark-skin-like patterned film. Reproduced from reference [111].

To manufacture transparent self-cleaning SHPo surfaces, the bottom-up method based on self-assembly of colloidal silica NPs could be more advantageous than the top-down one using plasma etching or soft lithography (nanoimprint lithography, replication) [112]. The former is more suitable for low-cost mass-production of various rough substrates, while the latter provides a well-defined size and shape of surface structures. In the former case, the size and surface chemistry of NPs should be finely controlled to balance the forces in colloidal systems, which determine the film morphology and uniformity after dip, spin or spray coating. A stable SHPo surface with hierarchical arrays could be fabricated by two-step self-assembly of colloidal silica NPs and surface functionalization with fluorosilane. Non-close-packed (NCP) colloidal multilayers were first spin-coated, and then uniform NPs were assembled on the NCP microspheres by second spin coating [113].

Spray coating is a facile and cheap method, which can be easily applied to any substrate and used even for consumer applied coating. A transparent superoleophobic surface was spray-coated in one step with a solution of stringed amphiphilic silica NPs in amphiphilic sol [114]. The stringed NPs formed a fractal-like nanoporous network while the sol acted as surface modifier and binder to enhance the coating durability against heating (up to 400 °C), water jetting and sand abrasion. Spray-coating of durable SHPo composite films usually requires harsh or volatile organic solvents for solution processing of polymers and dispersing hydrophobic NPs. The replacement of

harmful organic solvents with water can enhance the scalability of spray-coating without the increased cost in chemical handling and environmental safety concerns. An environment-friendly method of spray coating was developed with a water-based solution, which was comprised of exfoliated graphite nanoplatelets (xGnPs), polyolefin (PE) dispersion and ammonium hydroxide [115]. In this method, hydrophobic components (xGnPs) could be stabilized in water by utilizing chemicals containing acid functional groups (acrylic acid), which can become ionized in aqueous environments under proper pH control (pH > 7). The PE dispersion contained polyethylene-acrylic acid copolymer (～40%) and ammonium hydroxide (used as a pH adjuster). After spray coating and drying at 80 °C for 1 hour, the xGnPs became water insoluble to promote liquid repellency.

3.4.3. Multifunctionality

Multifunctionality is another important requirement for increasing product value and expanding applications of structured surfaces with engineered wettability. Self-cleaning coatings for optical applications would require high transparency for visible light and self-cleaning ability for long service life. However, it may be difficult to combine a specific wettability designed for a specific application with other desired functions. For example, surface roughness is beneficial to enhance or reduce wettability but will likely increase light scattering. Thus, to fabricate desired wetting surfaces that satisfy multiple functionalities, materials, structures and processes should be designed by simultaneously considering their effects on different functionalities. Antireflective self-cleaning coatings could be generally fabricated by using sub-100 nm surface roughness as

well as a transparent material (ceramics or polymers) [116,117]. Many research works have been conducted to develop multifunctional coatings and textiles based on specifically prescribed wettability. An antireflective, self-cleaning and antifogging film was deposited on glass substrate by sol-gel coating of oxide double-layers for application of photovoltaic cells [118]. The bottom layer of a hybrid methyl-functionalized nanoporous SiO_2 exhibited high transparency (antireflective), high water repellency and high mechanical stability. The top layer of an ultrathin nanoperforated TiO_2 imparted high water wettability (for antifogging) and photocatalysis (for self-cleaning) on the surface. The thicknesses and refractive indices of two layers were controlled to adjust the antireflectivity in the visible wavelength range. A free-standing transparent stretchable and SHPo composite film was fabricated by two-step spraying of resin and SHPo silica NP paint, followed by subsequent demolding of the resin composite paint [119]. It could sustain the SHPo property after straining (up to 100%), immersing in various corrosive liquids, pollution by sludge water, sandpaper abrasion and heat treatment (at 150 °C for 24 h) due to its multifunctional properties of anticorrosion, self-cleaning and mechanical/thermal stability.

A self-cleaning, antibacterial and UV protective textile was fabricated from a polyester/wool fabric by enzymatic pretreatment to hydrolyze the fabric surface and was followed by dip coating with TiO_2 NPs and cross-linking agent of butane tetracarboxylic acid (BTCA) [120]. The self-cleaning and antibacterial properties were verified by color removal from the stained fabric and by inhibited growth of gram-negative bacteria (E. coli). A flame-retardant, self-healing and waterproof film was dip-coated on cotton fabric with a trilayer of branched poly(ethylenimine)

(bPEI), ammonium polyphosphate (APP) and F-POSS [121]. When directly exposed to flame, the trilayer coating generated a porous surface layer of char (residual black carbon material) to give a self-extinguishing property. It could repeatedly restore its SHPo property after O_2 plasma etching by just keeping in a slightly humid environment (with a relative humidity of 35%) for 1 hour. Furthermore, it could endure more than 1000 cycles of abrasion with metal under a pressure of 44.8 kPa without losing the flame retardancy and self-healing SHPo properties.

In order to achieve multifunctionality, surfaces are commonly designed with sophisticated structures and chemical heterogeneity, but it is difficult to secure their mechanical durability and develop scale-up fabrication for industrial production. Therefore, it is important to obtain a proper combination of design simplicity and multifunctional performances for successful commercialization.

3.5. Conclusions

The research activities on structured surfaces of controlled wettability have been increasing rapidly, and researchers have made great progress so far in applied technology as well as basic science. Nowadays, SHPi or SHPo surface can be obtained on any substrate (metal, ceramic, polymer or textile) by nanotechnology-based surface modification or coating, and SHPi or SHPo regions can be placed on a given substrate in a desired pattern. In addition, major application areas of certain wettable surfaces have been explored, including self-cleaning, antifouling, anticorrosion and oil-water separation. In another application field, biomedical devices have also been explored,

such as contactless liquid handling platform for biomedical analyses, controlled-release drug delivery system and simple low-cost microfluidics for POCT.

Meanwhile, significant commercialization has been achieved mainly in self-cleaning and antifouling fields, although there still are common challenges for practical applications, such as mechanical durability, scalable manufacturing and multifunctionality. In general, the first two are essential to secure long-term performance and cost competitiveness for commercial products, and the last one is optional to promote the product value. It is highly recommended to review the existing research outcomes in order to advance the technologies of wettability engineering for successful commercialization in the future. For this purpose, it is helpful to understand which technologies are promising for each application and to analyze their relative competitiveness against existing products. For self-cleaning applications, TiO_2-based SHPi coatings are more extensively used than SiO_2-based SHPo ones due to their multifunctionality such as deodorizing and antibacterial performances. For marine application, PDMS-based SHPo antifouling coatings are accepted more than PEG-based SHPi ones due to their higher performance in the normal conditions of water flows. However, for biomedical application, the PEG-based SHPi surface seems to be better due to the higher resistance to irreversible, nonspecific absorption of proteins. Among many SHPo anticorrosion coatings, the best one appears to be based on polymer/inorganic NP composite (such as PTFE/SiO_2 and PU/Al_2O_3) due to the relatively high mechanical durability and environmental friendliness. However, to date there has not been research work that demonstrates its superiority over existing products.

References

1. Nishino T, Meguro M, Nakamae K, Matsushita M, Ueda Y. The Lowest Surface Free Energy Based on -CF3 Alignment. Langmuir. 1999; 15: 4321-3.
2. Chen Z, Nosonovsky M. Revisiting lowest possible surface energy of a solid. Surface Topography: Metrology and Properties. 2017; 5: 045001.
3. Onda T, Shibuichi S, Satoh N, Tsujii K. Super-Water-Repellent Fractal Surfaces. Langmuir. 1996; 12: 2125–2127.
4. Quéré D. Wetting and Roughness. Annual Review of Materials Research. 2008; 38: 71–99.
5. Marmur A. Non-Wetting Fundamentals. In: Ras RHA and Marmur A, editors. Non-wettable Surfaces: Theory, Preparation, and Applications. Cambridge: The Royal Society of Chemistry; 2016. pp. 1-11.
6. Hollebone B. Oil Physical Properties: Measurement and Correlation. In: Fingas M, editors. Oil Spill Science and Technology. 2nd ed. Oxford: Elsevier; 2017. pp. 185–208.
7. Tuteja A, Choi W, Ma M, Mabry JM, Mazzella SA, Rutledge GC, McKinley GH, Cohen RE. Designing Superoleophobic Surfaces. Science. 2007; 318: 1618–22
8. Liu T, Kim C-J. Turning a surface superrepellent even to completely wetting liquids. Science. 2014; 346: 1096–100.
9. Li F, Wang Z, Huang S, Pan Y, Zhao X. Flexible, Durable, and Unconditioned Superoleophobic/Superhydrophilic Surfaces for Controllable Transport and Oil–Water Separation. Adv Funct Mater. 2018; 28: 1706867.

10. Young T. An Essay on the Cohesion of Fluids. Phil Trans R Soc. 1805; 95: 65-87.

11. Wenzel RN. RESISTANCE OF SOLID SURFACES TO WETTING BY WATER. Ind Eng Chem Res. 1936; 28: 988–94.

12. Cassie ABD, Baxter S. WETTABILITY OF POROUS SURFACES. Trans Faraday Soc. 1944; 40: 546-51.

13. Marmur A. Wetting on Hydrophobic Rough Surfaces: To Be Heterogeneous or Not To Be? Langmuir. 2003; 19: 8343–8.

14. Dussan EB, Chow RTP. On the ability of drops or bubbles to stick to non-horizontal surfaces of solids. J Fluid Mech. 1983; 137: 1–29.

15. Eral HB, ′t Mannetje DJCM, Oh JM. Contact angle hysteresis: A review of fundamentals and applications. Colloid Polym Sci. 2013; 291: 247–60.

16. Olveira S, Stojanovic A, Seeger S. Superhydrophilic and Superamphiphilic Coatings. In: Wu L, Baghdachi J, editors. Functional Polymer Coatings Principles, Methods, and Applications. New Jersey: John Wiley & Sons; 2015. pp. 96–132.

17. Im M, Im H, Lee J-H, Yoon J-B, Choi Y-K. A robust superhydrophobic and superoleophobic surface with inversetrapezoidal microstructures on a large transparent flexible substrate. Soft Matter. 2010; 6: 1401–4.

18. Guo F, Guo Z. Inspired smart materials with external stimuli responsive wettability: a review. RSC Adv. 2016; 6: 36623–41.

19. Buten C, Kortekaas L, Ravoo BJ. Design of Active Interfaces Using Responsive Molecular Components. Adv Mater. 2019; 1904957.

20. Liu H, Wang Y, Huang J, Chen Z, Chen G, Lai Y. Bioinspired Surfaces with Superamphiphobic Properties: Concepts, Synthesis, and Applications. Adv Funct Mater. 2018; 28: 1707415

21. Li X-M, Reinhoudt D, Crego-Calama M. What do we need for a superhydrophobic surface? A review on the recent progress in the preparation of superhydrophobic surfaces. Chem Soc Rev. 2007; 36: 1350–68.

22. Ragesh P, Ganesh VA, Nair SV, Nair AS. A review on 'self-cleaning and multifunctional materials'. J Mater Chem A. 2014; 2: 14773–97.

23. Taikum O, Friehmelt R, Scholz M, Degussa E. The last 100 years of fumed silica in rubber reinforcement. In: The Free Library. 2010. https://www.thefreelibrary.com/The+last+100+years+of+fumed+silica+in+rubber+reinforcement.-a0238750507. (Last Accessed Date: 27 Dec 2019).

24. Latthe SS, Sutar RS, Kodag VS, Bhosale AK, Kumar AM, Sadasivuni KK, Xing R, Liu S. Self-cleaning superhydrophobic coatings: Potential industrial applications. Prog Org Coat. 2019; 128: 52–8.

25. Montazer M, Pakdel E. Functionality of nano titanium dioxide on textiles with future aspects: Focus on wool. J Photochem Photobiol C Photochem Rev. 2011; 12; 293–303.

26. Banerjee S, Dionysiou DD, Pillai SC. Self-cleaning applications of TiO2 by photo-induced hydrophilicity and photocatalysis. Appl Catal B Environ. 2015; 176: 396–428.

27. Yadav HM, Kim J-S, Pawar SH. Developments in photocatalytic antibacterial activity of nano TiO_2: A review. Korean J Chem Eng. 2016; 33: 1989–98.

28. Bressy C, Lejars MN. Marine Fouling : An Overview. J Ocean Technol. 2014; 9: 19–28.

29. Salta M, Wharton JA, Stoodley P, Dennington SP, Goodes LR, Werwinski S, Mart U, Wood RJK, Stokes KR. Designing biomimetic antifouling surfaces. Philos Trans R Soc A. 2010; 368: 4729–54.

30. Nurioglu AG, Esteves ACC. de With G. Non-toxic, non-biocide-release antifouling coatings based on molecular structure design for marine applications. J Mater Chem B. 2015; 3: 6547–70.

31. Brady JR RF, Singer IL. Mechanical Factors Favoring Release from Fouling Release Coatings. Biofouling. 2000; 15: 73–81.

32. Lejars M, Margaillan A, Bressy C. Fouling Release Coatings: A Nontoxic Alternative to Biocidal Antifouling Coatings. Chem Rev. 2012; 112: 4347–90.

33. Zander ZK, Becker ML. Antimicrobial and Antifouling Strategies for Polymeric Medical Devices. ACS Macro Lett. 2018; 7: 16–25.

34. Healthcare-Acquired Infections (HAIs). In: Patient CareLink. https://patientcarelink.org/improving-patient-care/healthcare-acquired-infections-hais/. (Last Accessed Date: 27 Dec 2019).

35. Belhadjamor M, Mansori ME, Belghith S, Mezlini S. Anti-fingerprint properties of engineering surfaces: a review. Surf Eng. 2018; 34: 85–120.

36. Min K, Han J, Park B, Cho E. Characterization of Mechanical Degradation in Perfluoropolyether Film for Its Application to Antifingerprint Coatings. ACS Appl Mater Interfaces. 2018; 10: 37498–506.

37. Koch G, Varney J, Thompson N, Moghissi O, Gould M, Payer J, Bowman E. International Measures of Prevention, Application, and Economics of Corrosion Technologies Study. Houston: NACE International; 2016.

38. Raja PB, Sethuraman MG. Natural products as corrosion inhibitor for metals in corrosive media - A review. Mater Lett. 2008; 62: 113–6.

39. Sørensen PA, Kiil S, Dam-Johansen K, Weinell CE. Anticorrosive coatings: a review. J Coat Technol Res. 2009; 6: 135–76.

40. Tiwari A. Anticorrosion Coating Industry Transitioning to Sustainable Development. In: PCI Paint & Coatings Industry 2017. https://www.pcimag.com/articles/103192-anticorrosion-coating-industry-transitioning-to-sustainable-development. (Last Accessed Date: 27 Dec 2019).

41. Wang Z, Li Q, She Z, Chen F, Li L, Zhang X, Zhang P. Facile and fast fabrication of superhydrophobic surface on magnesium alloy. Appl Surf Sci. 2013; 271: 182–92.

42. Wu L-K, Zhang X-F, Hu J-M. Corrosion protection of mild steel by one-step electrodeposition of superhydrophobic silica film. Corros Sci. 2014; 85: 482–7.

43. Calabrese L, Bonaccorsi L, Caprì A, Proverbio E. Adhesion aspects of hydrophobic silane zeolite coatings for corrosion protection of aluminium substrate. Prog Org Coat. 2014; 77: 1341–50.

44. Wang H, Chen E, Jia X, Liang L, Wang Q. Superhydrophobic coatings fabricated with polytetrafluoroethylene and SiO2 nanoparticles by spraying process on carbon steel surfaces. Appl Surf Sci. 2015; 349: 724–32.

45. Chen X, Yuan J, Huang J, Ren K, Liu Y, Lu S, Li H. Large-scale fabrication of superhydrophobic polyurethane/nano-Al2O3 coatings by suspension flame spraying for anti-corrosion applications. Appl Surf Sci. 2014; 311: 864–9.

46. Chang K-C, Hsu M-H, Lu H-I, Lai M-C, Liu P-J, Hsu C-H, Ji W-F, Chuang T-L, Wei Y, Yeh J-M, Liu W-R. Room-temperature cured hydrophobic epoxy/graphene composites as corrosion inhibitor for cold-rolled steel. Carbon. 2014; 66: 144–53.

47. Sebastian D, Yao C-W, Lian I. Mechanical Durability of Engineered Superhydrophobic Surfaces for Anti-Corrosion. Coatings. 2018; 8: 162.

48. Montemor MF. Functional and smart coatings for corrosion protection: A review of recent advances. Surf Coat Technol. 2014; 258: 17–37.

49. Xue Z, Cao Y, Liu N, Feng L, Jiang L. Special wettable materials for oil/water separation. J Mater Chem A. 2014; 2: 2445–60.

50. Gupta RK, Dunderdale GJ, England MW, Hozumi A. Oil/water separation techniques: a review of recent progresses and future directions. J Mater Chem A. 2017; 5: 16025–58.

51. Yong J, Huo J, Chen F, Yang Q, Hou X. Oil/water separation based on natural materials with super-wettability: recent advances. Phys Chem Chem Phys. 2018; 20: 25140–163.

52. Yong J, Chen F, Yang Q, Huo J, Hou X. Superoleophobic surfaces. Chem Soc Rev. 2017; 46: 4168–217.

53. Xue Z, Wang S, Lin L, Chen L, Liu M, Feng L, Jiang L. A Novel Superhydrophilic and Underwater Superoleophobic Hydrogel-Coated Mesh for Oil/Water Separation. Adv Mater. 2011; 23: 4270–3.

54. Teng C, Lu X, Ren G, Zhu Y, Wan M, Jiang L. Underwater Self-Cleaning PEDOT-PSS Hydrogel Mesh for Effective Separation of Corrosive and Hot Oil/Water Mixtures. Adv Mater Interfaces. 2014; 1: 1400099.

55. Yang J, Zhang Z, Xu X, Zhu X, Men X, Zhou X. Superhydrophilic–superoleophobic coatings. J Mater Chem. 2012; 22: 2834–7.

56. Zhu Y, Wang D, Jiang L, Jin J. Recent progress in developing advanced membranes for emulsified oil/water separation. NPG Asia Materials. 2014; 6: e101.

57. Zhang W, Shi Z, Zhang F, Liu X, Jin J, Jiang L. Superhydrophobic and Superoleophilic PVDF Membranes for Effective Separation of Water-in-Oil Emulsions with High Flux. Adv Mater. 2013; 25: 2071–6.

58. Zhu Y, Zhang F, Wang D, Pei XF, Zhang W, Jin J. A novel zwitterionic polyelectrolyte grafted PVDF membrane for thoroughly separating oil from water with ultrahigh efficiency. J Mater Chem A. 2013; 1: 5758–65.

59. Ju J, Wang T, Wang Q. Superhydrophilic and underwater superoleophobic PVDF membranes via plasma-induced surface PEGDA for effective separation of oil-in-water emulsions. Colloids Surf A. 2015; 481: 151–7.

60. Zhu Q, Pan Q, Liu F. Facile Removal and Collection of Oils from Water Surfaces through Superhydrophobic and Superoleophilic Sponges. J Phys Chem C, 2011; 115: 17464–70.

61. Ke Q, Jin Y, Jiang P, Yu J. Oil/Water Separation Performances of Superhydrophobic and Superoleophilic Sponges. Langmuir. 2014; 30: 13137–42.

62. Li X, Xue Y, Zou M, Zhang D, Cao A, Duan H. Direct Oil Recovery from Saturated Carbon Nanotube Sponges. ACS Appl Mater Interfaces. 2016; 8: 12337–43.

63. Bi H, Yin Z, Cao X, Xie X, Tan C, Huang X, Chen B, Chen F, Yang Q, Bu X, Lu X, Sun L, Zhang H. Carbon Fiber Aerogel Made from Raw Cotton: A Novel, Efficient and Recyclable Sorbent for Oils and Organic Solvents. Adv Mater. 2013; 25: 5916–21.

64. Sun H, Xu Z, Gao C. Multifunctional, Ultra-Flyweight, Synergistically Assembled Carbon Aerogels. Adv Mater. 2013; 25: 2554–60.

65. Mu L, Yang S, Hao B, Ma P-C. Ternary Silicone Sponge with Enhanced Mechanical Properties for Oil–Water Separation. Polym Chem. 2015; 6: 5869–75.

66. Zhang Y, Wei S, Liu F, Du Y, Liu S, Ji Y, Yokoi T, Tatsumi T, Xiao F-S. Superhydrophobic nanoporous polymers as efficient adsorbents for organic compounds. Nanotoday. 2009; 4: 135–42.

67. Yu Y, Wu X, Fang J. Superhydrophobic and superoleophilic ‘‘sponge-like’’ aerogels for oil/water separation. J Mater Sci. 2015; 50: 5115–24.

68. Yu S, Tan H, Wang J, Liu X, Zhou K. High Porosity Supermacroporous Polystyrene Materials with Excellent Oil–Water Separation and Gas Permeability Properties. ACS Appl Mater Interfaces. 2015; 7: 6745–53.

69. Yang C, Kaipa U, Mather QZ, Wang X, Nesterov V, Venero AF, Omary MA. Fluorous Metal-Organic Frameworks with Superior Adsorption and Hydrophobic Properties toward Oil Spill Cleanup and Hydrocarbon Storage. J Am Chem Soc. 2011; 133: 18094–7.

70. Mishra P, Balasubramanian K. Nanostructured Microporous Polymer Composite Imprinted with Superhydrophobic Camphor Soot, for Emphatic Oil–Water Separation. RSC Adv. 2014; 4: 53291–6.

71. Korhonen JT, Kettunen M, Ras RHA, Ikkala O. Hydrophobic Nanocellulose Aerogels as Floating, Sustainable, Reusable, and Recyclable Oil Absorbents. ACS Appl Mater Interfaces. 2011; 3: 1813–6.

72. Cervin NT, Aulin C, Larsson PT, Wågberg L. Ultra porous nanocellulose aerogels as separation medium for mixtures of oil/water liquids. Cellulose. 2012; 19: 401–10.

73. Ciasca G, Papi M, Businaro L, Campi G, Ortolani M, Palmieri V, Cedola A, De Ninno A, Gerardino A, Maulucci G, De Spirito M. Recent advances in superhydrophobic surfaces and their relevance to biology and medicine. Bioinspir Biomim. 2016; 11: 011001.

74. Tuckermann R, Puskar L, Zavabeti M, Sekine R, McNaughton D. Chemical analysis of acoustically levitated drops by Raman spectroscopy. Anal Bioanal Chem. 2009; 394: 1433–41.

75. Tsujino S, Tomizaki T. Ultrasonic acoustic levitation for fast frame rate X-ray protein crystallography at room temperature. Sci Rep. 2016; 6: 25558.

76. Ciasca G, Businaro L, De Ninno A, Cedola A, Notargiacomo A, Campi G, Papi M, Ranieri A, Carta S, Giovine E, Gerardino A. Wet sample confinement by superhydrophobic patterned surfaces for combined X-ray fluorescence and X-ray phase contrast imaging. Microelectron Eng. 2013; 111: 304–9.

77. Gentile F, Coluccio ML, Coppedè N, Mecarini F, Das G, Liberale C, Tirinato L, Leoncini M, Perozziello G, Candeloro P, De Angelis F, Di Fabrizio E. Superhydrophobic Surfaces as Smart Platforms for the Analysis of Diluted Biological Solutions. ACS Appl Mater Interfaces. 2012; 4: 3213–24.

78. Lima AC, Mano, JF. Micro/nano-structured superhydrophobic surfaces in the biomedical field: part II: applications overview. Nanomedicine (Lond.). 2015; 10: 271–97.

79. Ueda E, Geyer FL, Nedashkivska V, Levkin PA. Droplet Microarray: facile formation of arrays of microdroplets and hydrogel micropads for cell screening applications. Lab Chip. 2012; 12: 5218–24.

80. Neto AI, Custódio CA, Song W, Mano JF. High-throughput evaluation of interactions between biomaterials, proteins and cells using patterned superhydrophobic substrates. Soft Matter. 2011; 7: 4147–51.

81. Popova AA, Demir K, Hartanto TG, Schmitt E, Levkin PA. Droplet-Microarray on Superhydrophobic-Superhydrophilic Patterns for High-Throughput Live Cell Screenings. RSC Adv. 2016; 6: 38263–76.

82. Luz GM, Leite ÁJ, Neto AI, Song W, Mano JF. Wettable arrays onto superhydrophobic surfaces for bioactivity testing of inorganic nanoparticles. Mater Lett. 2011; 65: 296–9.

83. Liu D, Yang F, Xiong F, Gu N. The Smart Drug Delivery System and Its Clinical Potential. Theranostics. 2016; 6: 1306–23.

84. Yohe ST, Colson YL, Grinstaff MW. Superhydrophobic Materials for Tunable Drug Release: Using Displacement of Air to Control Delivery Rates. J Am Chem Soc. 2012; 134: 2016–9.

85. Chou S-F, Carson D, Woodrow KA. Current strategies for sustaining drug release from electrospun nanofibers. J Control Release. 2015; 220: 584–91.

86. Chenab KK, Sohrabi B, Rahmanzadeh A. Superhydrophobicity: advanced biological and biomedical applications. Biomater Sci. 2019; 7: 3110–37.

87. Gui W, Lin J, Hao G, Liang Y, Wang W, Wen Y. Light-Triggered Drug Release Platform Based on Superhydrophobicity of Mesoporous Silica Nanoparticles. Nanosci Nanotechnol Lett. 2016; 8: 428–33.

88. Zhou J, Frank MA, Yang Y, Boccaccini AR, Virtanen S. A novel local drug delivery system: Superhydrophobic titanium oxide nanotube arrays serve as the drug reservoir and ultrasonication functions as the drug release trigger. Mater Sci Eng C. 2018; 82: 277–83.

89. Lee C, Choi C-H, Kim C-J. Superhydrophobic drag reduction in laminar flows: a critical review. Exp Fluids. 2016; 57: 176.

90. Ellinas K, Tserepi A, Gogolides E. Superhydrophobic, passive microvalve with controllable opening threshold: exploiting plasma nanotextured microfluidics for a programmable flow switchboard. Microfluid Nanofluid. 2014; 17: 489–98.

91. Oliveira NM, Vilabril S, Oliveira MB, Reis RL, Mano JF. Recent advances on open fluidic systems for biomedical applications: A review. Mater Sci Eng C. 2019; 97: 851–63.

92. Oliveira NM, Neto AI, Song W, Mano JF. Two-Dimensional Open Microfluidic Devices by Tuning the Wettability on Patterned Superhydrophobic Polymeric Surface. Appl Phys Express. 2010; 3: 085205.

93. Obeso CG, Sousa MP, Song W, Rodriguez-Pérez MA, Bhushan B, Mano JF. Modification of paper using polyhydroxybutyrate to obtain biomimetic superhydrophobic substrates. Colloids Surf A. 2013; 416: 51–5.

94. You I, Kang SM, Lee S, Cho YO, Kim JB, Lee SB, Nam YS, Lee H. Polydopamine Microfluidic System toward a Two-Dimensional, Gravity-Driven Mixing Device. Angew Chem Int Ed. 2012; 124: 6230–4.

95. Nguyen N-T, Hejazian M, Ooi CH, Kashaninejad N. Recent Advances and Future Perspectives on Microfluidic Liquid Handling. Micromachines. 2017; 8: 186.

96. Nelson WC, Kim C-J. Droplet Actuation by Electrowetting-on-Dielectric (EWOD): A Review. J Adhes Sci Technol. 2012; 26: 1747–71.

97. Kavousanakis ME, Chamakos NT, Ellinas K, Tserepi A, Gogolides E, Papathanasiou AG. How to Achieve Reversible Electrowetting on Superhydrophobic Surfaces. Langmuir. 2018; 34: 4173–9.

98. Milionis A, Loth E, Bayer IS. Recent advances in the mechanical durability of superhydrophobic materials. Adv Colloid Interface Sci. 2016; 229: 57–79.

99. Verho T, Bower C, Andrew P, Franssila S, Ikkala O, Ras RHA. Mechanically Durable Superhydrophobic Surfaces. Adv Mater. 2011; 23: 673–8.

100. Mortazavi V, Khonsari MM. On the degradation of superhydrophobic surfaces: A review. Wear. 2017; 372–373: 145–57.

101. Bayer IS, Brown A, Steele A, Loth E. Transforming Anaerobic Adhesives into Highly Durable and Abrasion Resistant Superhydrophobic Organoclay Nanocomposite Films: A New Hybrid Spray Adhesive for Tough Superhydrophobicity. Appl Phys Express. 2009; 2: 125003.

102. Zhou H, Wang H, Niu H, Gestos A, Wang X, Lin T. Fluoroalkyl Silane Modified Silicone Rubber/Nanoparticle Composite: A Super Durable, Robust Superhydrophobic Fabric Coating. Adv Mater. 2012; 24: 2409–12.

103. Xiu Y, Liu Y, Hess DW, Wong CP. Mechanically robust superhydrophobicity on hierarchically structured Si surfaces. Nanotechnology. 2010; 21: 155705.

104. Zimmermann J, Reifler FA, Fortunato G, Gerhardt L-C, Seeger S. A Simple, One-Step Approach to Durable and Robust Superhydrophobic Textiles. Adv Funct Mater. 2008; 18: 3662–9.

105. Li Y. Li L, Sun J. Bioinspired Self-Healing Superhydrophobic Coatings. Angew Chem Int Ed. 2010; 49: 6129–33.

106. Qian H, Xu D, Du C, Zhang D, Li X, Huang L, Deng L, Tu Y, Mol JMC, Terryn HA. Dual-action smart coatings with a self-healing superhydrophobic surface and anti-corrosion properties. J Mater Chem A. 2017; 5: 2355–64.

107. Jung YC, Bhushan B. Mechanically Durable Carbon Nanotube–Composite Hierarchical Structures with Superhydrophobicity, Self-Cleaning, and Low-Drag. ACS Nano. 2009; 3: 4155–63.

108. Xue C-H, Zhang Z-D, Zhang J, Jia S-T. Lasting and Self-Healing Superhydrophobic Surfaces by Coating of Polystyrene/SiO2 Nanoparticles and Polydimethylsiloxane. J Mater Chem A. 2014; 2: 15001–7.

109. Cooper K. Scalable Nanomanufacturing – A Review. Micromachines. 2017; 8: 20.

110. Li Y, John J, Kolewe KW, Schiffman JD, Carter KR. Scaling Up Nature: Large Area Flexible Biomimetic Surfaces. ACS Appl Mater Interfaces. 2015; 7: 23439–44.

111. Park S-H, Lee S, Moreira D, Bandaru PR, Han IT, Yun D-J. Bioinspired superhydrophobic surfaces, fabricated through simple and scalable roll-to-roll processing. Sci Rep. 2015; 5: 15430.

112. Rahmawan Y, Xu L, Yang S. Self-assembly of nanostructures towards transparent, superhydrophobic surfaces. J Mater Chem A. 2013; 1: 2955–69.

113. Yang H, Jiang P. Scalable fabrication of superhydrophobic hierarchical colloidal arrays. J Colloid Interface Sci. 2010; 352: 558–65.

114. Ge D, Yang L, Zhang Y, Rahmawan Y, Yang S. Transparent and Superamphiphobic Surfaces from One-step Spray Coating of Stringed Silica Nanoparticle/Sol Solutions. Part Part Sys Charact. 2014; 31: 763–70.

115. Schutzius TM, Bayer IS, Qin J, Waldroup D, Megaridis CM. Water-Based, Nonfluorinated Dispersions for Environmentally Benign, Large-Area, Superhydrophobic Coatings. ACS Appl Mater Interfaces. 2013; 5: 13419–25.

116. Karunakaran RG, Lu C-H, Zhang Z, Yang S. Highly Transparent Superhydrophobic Surfaces from the Coassembly of Nanoparticles (≤ 100 nm). Langmuir. 2011; 27: 4594–602.

117. Bayer IS. On the Durability and Wear Resistance of Transparent Superhydrophobic Coatings. Coatings. 2017; 7: 12.

118. Faustini M, Nicole L, Boissière C, Innocenzi P, Sanchez C, Grosso D. Hydrophobic, Antireflective, Self-Cleaning, and Antifogging Sol-Gel Coatings: An Example of

Multifunctional Nanostructured Materials for Photovoltaic Cells. Chem Mater. 2010; 22: 4406–13.

119. Wang S, Yu X, Zhang Y. Large-scale fabrication of translucent, stretchable and durable superhydrophobic composite films. J Mater Chem A. 2017; 5: 23489–96.

120. Montazer YM, Seifollahzadeh S. Enhanced Self-cleaning, Antibacterial and UV Protection Properties of Nano TiO_2 Treated Textile through Enzymatic Pretreatment. Photochem Photobiol. 2011; 87: 877–83.

121. Chen S, Li X, Li Y, Sun J. Intumescent Flame-Retardant and Self-Healing Superhydrophobic Coatings on Cotton Fabric. ACS Nano. 2015; 9: 4070–6.